Determining the influence of a pivot to center-of-mass distance on the time period of an oscillation in a compound pendulum

Luna Pestotnik Stres

Stres InŽeniring d.o.o.

Tip publikacije: Monografska publikacija
Naslov: Determining the influence of a pivot to center-of-mass distance on the time period of an oscillation in a compound pendulum
Avtor: Luna Pestotnik Stres
Leto izdaje: 2025
Jezik: angleški
Država izdaje: Slovenija
Kraj izdaje: Tolmin
Založnik: Stres Inženiring d.o.o.
Format: PDF
URL: https://stres-apartments.eu/books/monografija_FIZ.pdf

CIP:
Kataložni zapis o publikaciji (CIP) pripravili v Narodni in univerzitetni knjižnici v Ljubljani
COBISS.SI-ID 247678467
ISBN 978-961-93233-8-0 (PDF)

1. AIM AND RESEARCH QUESTION

This experiment aims to investigate how the pivot distance from the centre-of-mass influences the time period of oscillation in a compound pendulum at small angles. A stopwatch is used to obtain the time measurement.

Research question: *How does increasing the distance of the axis of rotation (1.3 cm,2.6 cm, 3.9 cm, 5.2 cm, 6.5 cm) from the mass centre of a rigid body of length l of 14.0cm affect the time period of oscillation (s) as observed through time measurements of 10 oscillations?*

2. INTRODUCTION

A while ago, while searching the internet, I stumbled upon an interesting video featuring the mechanism of the first clock to have a compound pendulum integrated into its design, the so-called "Clock 32" ("Brian Law's woodenclocks"). This clock's mechanism relies on a simple harmonic motion of a rigid body inside the clock, which drives the movement of the clock's hand. By investigating if such a rigid body oscillates differently from an idealised point-like one, I realised that laws of the simple harmonic oscillator can also be applied here. However, the motion of the rigid body is also crucially influenced by its moment of inertia. As I wanted to deepen my understanding of rigid body oscillations, I chose to investigate the nature of the movement of compound pendulums.

3. BACKGROUND INFORMATION

3.1 THEORETICAL BACKGROUND

Pendulums are freely oscillating devices suspended from the axis of rotation - the pivot. For point-like mass pendulums, the mass is concentrated at only one point. In such cases, the equation of motion can be described in terms of angular displacement θ as

$$\theta = \theta_0 \sin \frac{2\pi}{T_0} t \ , \qquad (1)$$

where t is time, θ_0 the amplitude of oscillations and T_0 the time period. T_0 can be derived as

$$T_0 = 2\pi \sqrt{\frac{l}{g}} \ , \qquad (2)$$

where l is the distance of the point-like mass pendulum from the pivot and g is the gravitational acceleration. However, most pendulums are compound pendulums, consisting of a rigid body (in this example, a rod), where the mass is distributed along the body's whole length. In such cases, its moment of inertia I, the tendency of the object to resist the change, has to be considered, as it changes with the centre-of-mass distance from the pivot.

In further analysis, a compound pendulum -the rod of mass m, length l and distance of centre-of-mass from the pivot d will be considered. Firstly, to derive the period of oscillation of this rod its free-body diagram is drawn to represent the forces acting on the system (Figure 1).

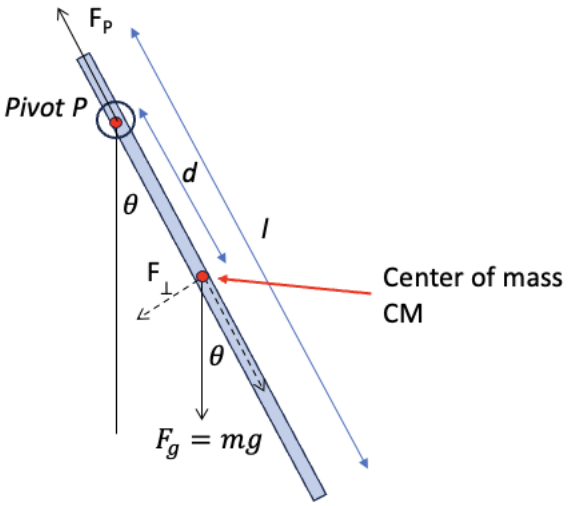

Figure 1: A free body diagram of forces (digitally drawn)

The gravitational force ($F_g = mg$) acting on the rod is represented at the centre of the rod's mass, where d is the distance between the pivot P and the center-of-mass (note that the weight acts on every rod segment). F_g can be decomposed into two components. The component acting in the direction of the rod $F_{g\parallel}$ is balanced by the force of the pivot Fp. The component acting perpendicular to the rod $F_{g\perp}$ is not balanced, resulting in a torque τ, $\tau = F_{g\perp} d$ on the pivot.
Using the trigonometric sine functions, acknowledging that the torque acts in the opposite direction than the increasing of θ, the total torque equals:

$$\tau = -mg \cdot d \sin\theta \quad . \tag{3}$$

According to the second Newton's law, the restoring torque results in angular acceleration α of the body ("Mujtaba"):

$$\tau = I \cdot \alpha \, , \tag{4}$$

where I is the moment of inertia. The two equations can be combined to obtain the relationship between I and d:

$$I \cdot \alpha = -\mathrm{mg} \cdot \mathrm{d} \sin\theta \quad . \tag{5}$$

Angular acceleration α is the second derivative of angular displacement θ, $\alpha = \frac{d^2\theta}{dt^2}$, thus

$$I \cdot \frac{d^2\theta}{dt^2} = -\mathrm{mg} \cdot \mathrm{d} \sin\theta \, . \tag{6}$$

This equation can be further rearranged to obtain:

$$\frac{d^2\theta}{dt^2} = \ddot{\theta} = -\frac{\mathrm{mg} \cdot \mathrm{d}}{I} \sin\theta. \tag{7}$$

For small angles θ ($\theta \ll 1$), the $\sin\theta$ can be replaced with θ.

$$\ddot{\theta} = -\frac{\mathrm{mg} \cdot \mathrm{d}}{I} \theta. \tag{8}$$

In Equation (8), we recognise the equation for a simple harmonic motion, with solutions for equations of motions shown in Table 1, where we identify $\frac{\mathrm{mg} \cdot \mathrm{d}}{I}$ as ω^2, where ω is the angular frequency.

Table 1: Derivations of equation for simple harmonic motion oscilating with ω

Equation of motion for θ	$\theta = \theta_0 \sin\omega t$
Equation of motion for angular velocity	$\dot{\theta} = \omega \, \theta_0 \cos\omega t$
Equation of motion for angular acceleration α	$\ddot{\theta} = -\omega^2 \theta_0 \sin\omega t$
Equation of motion in differential form	$\ddot{\theta} = -\omega^2 \theta$

$$\omega = \sqrt{\frac{mgd}{I}} \tag{9}$$

A time period of such a compound pendulum can therefore be written as:

$$T = \frac{2\pi}{\omega} = 2\pi\sqrt{\frac{I}{mgd}} \tag{10}$$

In the next step, the moment of inertia of a rod has to be derived. Considering first a system of mass particles m_i, composing the rod , the moment of inertia can be calculated as:

$$I = \sum_i m_i \, r_i{}^2 \ , \tag{11}$$

where r_i is the distance of each m_i from the pivot ("Moment of inertia"). Generalising this for a continuous rigid body – the rod- we replace the summation with the integral over the rod:

$$I = \int_{rod} r^2 dm \tag{12}$$

Again, *r* is the distance of the element *dm* from the pivot. Next, the rod's moment of inertia for pivot equals the center-of-mass (see Figure 2) is calculated. The linear mass density of such a rod is expressed as $\frac{m}{l}$. The coordinate system's origin is chosen to coincide with the pivot.

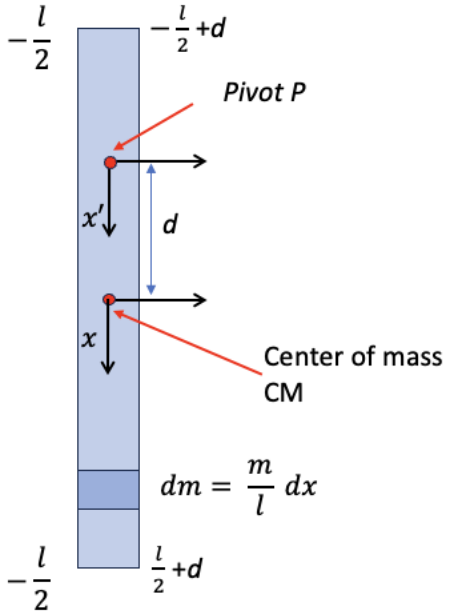

Figure 2: A rigid body with the rotation axis in the mass centre in the middle of the body

In this case, the moment of inertia *I* can be evaluated by integrating Equation 12 from - $\frac{l}{2}$ to $\frac{l}{2}$.

$$I = \int_{-\frac{l}{2}}^{\frac{l}{2}} r^2 dm \tag{13}$$

We express the infinitesimal element *dm* as
$dm = \frac{m}{l} dr$.
Inserting it into Equation 13, *I* around the center-of-mass in terms of length *l* can be calculated:

$$I_{CM} = \int_{-\frac{l}{2}}^{\frac{l}{2}} r^2 \frac{m}{l} dr = \frac{m}{l}\left(\frac{r^3}{3}\right)\Bigg|_{-\frac{l}{2}}^{\frac{l}{2}} = \frac{ml^2}{12} \quad (14)$$

For the pivot at a distance d from the center-of-mass, I can be calculated according to Equation 12 with correct integration limits. The origin of coordinate can be transformed as:

$$x' = x + d. \quad (15)$$

The moment of inertia is written as:

$$I = \int_{-\frac{l}{2}+d}^{\frac{l}{2}+d} r^2 \frac{m}{l} dr = \frac{m}{l}\left(\frac{r^3}{3}\right)\Bigg|_{-\frac{l}{2}+d}^{\frac{l}{2}+d} =$$

$$= \frac{m}{3l}\left(\left(\frac{l}{2}+d\right)^3 - \left(-\frac{l}{2}+d\right)^3\right)$$

$$I = \frac{ml^2}{12} + md^2 \quad (16)$$

The first term is recognised as the moment of inertia around the center-of-mass from Equation 14, so we can write I:

$$I = I_{CM} + md^2 \quad (17)$$

This expression has hereby been evaluated for a specific rod of length l; however, it holds for any rigid body and is known as Steiner's theorem ("Steiner's theorem").

3.2 THE VARIABLES

Independent variable: Pivot to center-of-mass distance *(1.3cm, 2.6cm, 3.9cm, 5.2cm, 6.5cm)*
Dependent variables: Time period (s)
Controlled variables:

Table 2: Controlled variables and explanations

Controlled variable	How is it controlled?	Why is it controlled?
Shape of the object	The same rigid body is used to obtain measurements	Changes in shape of the object would lead to different moment of inertia, changing the time period
Wind	The experiment is conducted in a controlled closed environment	Wind resistance could lead to disturbed measurements
Using the same pivot	Each time, the same pivot was used	Changing the pivot could lead to different frictions between the object and the pivot, distrupting the measurements
Starting amplitude	Each time, the object was released from the same small angle	At larger amplitudes, the system does not exhibit a simple harmonic motion

3.3 HYPOTHESIS

H_1: The period of oscillation will first decrease, reaching a minimum at a certain distance $d < l$, and then increase.
H_2: At large pivot to center-of-mass distances, the time period of a compound pendulum will approach time period of a simple point-like mass pendulum.

Equation 10 and 16 are considered for the creation of a hypothesis. Firstly, it can be predicted that the moment of inertia increases with increasing distance of the pivot from the center-of-mass, as the second term in its equation (md^2) increases. Secondly, the two equations are combined to obtain a time period T dependence on the distance of the pivot point.

$$T = 2\pi\sqrt{\frac{I}{mgd}} = 2\pi\sqrt{\frac{\frac{ml^2}{12} + md^2}{mgd}}$$

$$T = 2\pi\sqrt{\frac{l}{g}}\sqrt{\frac{l}{12d} + \frac{d}{l}} \tag{18}$$

In terms of a time period of a point-like mass pendulum (Equation 2), this can be written as

$$T(d) = T_0\sqrt{\frac{l}{12d} + \frac{d}{l}} \tag{19}$$

If $d \ll l$ the term $\frac{l}{12d}$ becomes dominant, $\frac{d}{l}$ approaches 0, and the relationship simplifies to $T \propto \sqrt{\frac{l}{12d}}$,
which goes to enormous values for tiny distances d.
If $d \gg l$, i.e., the pivot lies outside the rod, the second term prevails, and the first term becomes negligible. The behaviour in those two extremes suggests the existence of a minimum (turning point) in between.

3.4 MATERIALS AND EQUIPMENT

Table 3:Materials and equipment with precision of measurements

Material / equipment	*Characteristics and precision of measurement*
Thin steel pole	/
Adhesive tape	/
Stopwatch	± 0.01 s
Geotriangle	$\pm 2°$
A uniform iron rod with 11 equally distributed holes	$l = 14$ cm $\pm$ 0.1 cm, $m = 14$ g $\pm$ 1 g distance between two holes $= 1.3$ cm $\pm$ 0.1 cm

3.5 METHODOLOGY

The setup of the experiment is shown in Figure 3. The steel pole, acting as a pivot, is fixed to a table with adhesive tape. The iron rod is placed on the pivot, using different holes, displaced and left to oscillate from a small θ.

As the weight is equally distributed along the rod, its center-of-mass is determined as its middle, $d_{CM} = \frac{l}{2} = \frac{14.0\text{ cm}}{2} = 7.0$ cm. Since the holes are placed symmetrically relative to center-of-mass, the experiment is conducted using the holes on one side of the center-of-mass.

Due to friction in the pivot, the oscillations are damped, and the rod stopped after 5-15 oscillations. To increase the precision of the measurements, the time of 5-10 oscillations is measured and then divided by the number of oscillations.

Figure 3: Experimental setup (photos from private archive)

3.6 PROCEDURE

All the steps relate to the iron rod.

1. Measure the distance from each hole to its center-of-mass;
2. Hang it on the most outer hole;
3. Displace the rod for a small angle ($\theta = 10°$) using a geotriangle and release it to swing;
4. Turn on the stopwatch and measure the time of 10 oscillations (5 in the case of the innermost hole);
5. Repeat the measurements ten times;
6. Repeat 2.-5. for all the holes until the center-of-mass is reached.

3.6 SAFETY NOTES

Table 4: Safety notes

CONSIDERATION TYPE	SIGNIFICANCE
Environmental consideration	To limit the production of waste, the experiment setup comprised of materials which were already in use beforehand and their function returned to their original one after the experiment has ended. Moreover, the adhesive tape (the only material for a single use) was recycled appropriately.
Safety consideration	The setup of the experiment had to be assembled independently. Because of the sharpness of the iron rod, the experiment had to be conducted with causion to avoid any injuries.
Ethical considerations	There were no ethical considerations, as the experiment did not involve any human or animal participants.

4. RESULTS

4.1 QUALITATIVE OBSERVATIONS

During the procedure, changes in the time period were qualitatively observed. The time period was maximal at the pivot hole closest to the center-of-mass, and decreased over the successive two measurements. Due to the short and similar duration of the last three measurements, their time periods could not be qualitatively distinguished. For the pivot furthest from the center-of-mass at $d = 6.5$ cm the rod stopped after five oscillations due to friction related damping.

4.2 RAW DATA

During the experiment, ten trials were conducted at five different distances from the center-of-mass of the rod (Table 5). The trials aimed to determine the time period, and to minimise random error, therefore, the time for ten oscillations was recorded in all cases except for the distance d=1.3 cm, where the time for five measurements was obtained.

Table 5: Distance of the axis of rotation from the mass centre (d) and time period

d (cm) ±0.1cm	Number of oscillations	time (s) ±0.01s									
		T_1	T_2	T_3	T_4	T_5	T_6	T_7	T_8	T_9	T_{10}
1.3	5	3.74	3.69	3.62	3.63	3.76	3.79	3.53	3.54	3.75	3.51
2.6	10	6.04	5.87	5.87	5.91	6.01	5.94	5.88	5.66	5.74	5.81
3.9	10	5.65	5.73	5.46	5.58	5.43	5.49	5.68	5.58	5.66	5.64
5.2	10	5.66	5.76	5.63	5.76	5.70	5.63	5.63	5.88	5.61	5.79
6.5	10	5.89	6.06	5.89	6.01	5.80	6.10	6.00	5.79	6.06	6.14

5. DATA PROCESSING

First, the time period T was calculated by dividing each measured value by the number of oscillations. An example of calculation for $6.5\ \text{cm} \pm 0.1\ \text{cm}$, I for the first trial is shown below, and all the others can be seen in Table 6:

$$T = \frac{T_{10}}{10} = \frac{5.89s}{10} = 0.589s = 0.59s$$

Table 6: Time period for different axis distances

d (cm) ±0.1cm	time (s) ±0.01s									
	T_1	T_2	T_3	T_4	T_5	T_6	T_7	T_8	T_9	T_{10}
1.3	0.75	0.74	0.72	0.73	0.75	0.76	0.71	0.71	0.75	0.70
2.6	0.60	0.59	0.59	0.59	0.60	0.59	0.59	0.57	0.57	0.58
3.9	0.57	0.57	0.55	0.56	0.54	0.55	0.57	0.56	0.57	0.56
5.2	0.57	0.58	0.56	0.58	0.57	0.56	0.56	0.59	0.56	0.58
6.5	0.59	0.60	0.59	0.60	0.58	0.61	0.60	0.58	0.61	0.61

The raw data can now be used and represented on a graph in Figure 4.

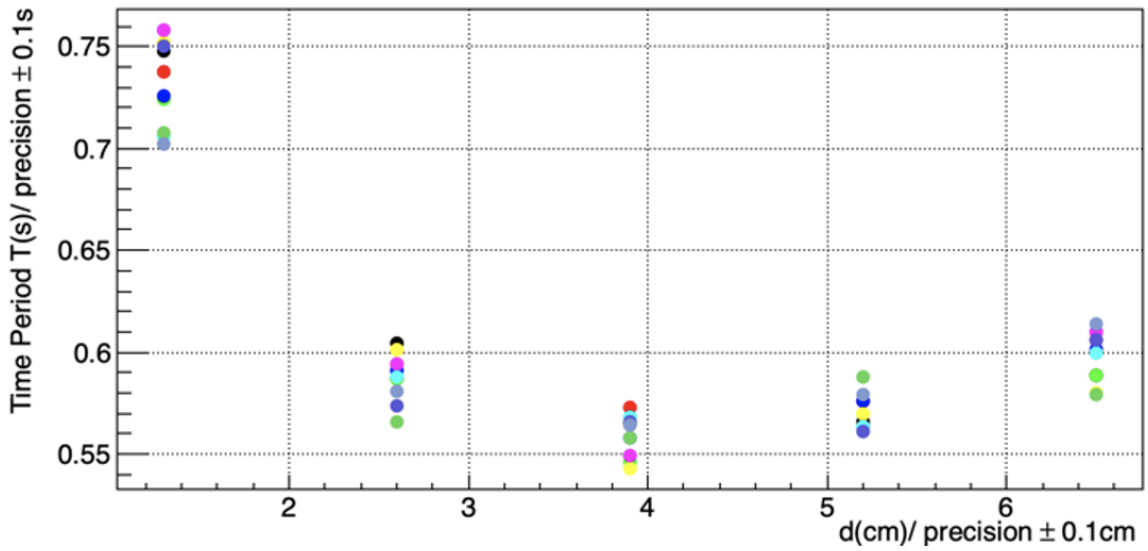

Figure 4: Raw data of the time period plotted on a graph.

A large fluctuation between the trials for the same pivot to center-of-mass distance can be noted as a first observation, no outliers are however observed. The values on the graph are dispersed, indicating a random measurement error. The average values and their absolute and relative uncertainties are determined to quantify the dispersion of the measurements. A sample of calculation for axis distance 6.5 cm $\pm$ 0.1 cm is shown below, and the remaining results of the calculations are presented in Table 7.

1. Calculating the average time period (T_{avg}):

$$T_{avg} = \frac{\sum_{i=1}^{10} T_i}{10}$$

$$T_{avg} = \frac{0.59\ s + 0.60\ \text{s} + 0.59\ \text{s} + \cdots + 0.61\ \text{s}}{10} = 0.597\ \text{s} = 0.60\ \text{s}$$

2. Calculating the absolute uncertainty of the time period (ΔT_{avg}):

$$\Delta T_{avg} = \frac{max - min}{2} = \frac{0.61\ \text{s} - 0.58\ \text{s}}{2} = 0.018\ \text{s} = 0.02\ \text{s}$$

3. Calculating the relative uncertainty:

$$\delta T_{avg} = \frac{\Delta T_{avg}}{T_{avg}} \cdot 100 = \frac{0.018}{0.597} = 3\ \%$$

4. Precision of the measurement can be evaluated from the distance and oscillation time measurements. The largest evaluated relative errors are found at the smallest measured distance, where 0.1 cm/ 1.3 cm approximates less than 8 %, and at the shortest measured time period, where 0.01 s/0.56 s approximates less than 2 %. The combined measurement error is therefore the sum of both, approximating to less than 10 %. All measurement errors are shown in Table 7 and Figure 5 as horizontal lines.

Table 7: Pivot distance, average time, absolute and relative uncertainties

$d\ (cm)$ ± 0.1	*Equipment uncertainty (d)*	$T_{avg}(s)$ ± 0.01	*Equipment uncertainty* (T_{avg})	$\Delta T_{avg}\ (s)$ ± 0.01	δT_{avg} (%)
1.3	0.077	0.73	0.014	0.03	4%
2.6	0.038	0.59	0.017	0.02	3%
3.9	0.026	0.56	0.018	0.02	3%
5.2	0.019	0.57	0.018	0.01	2%
6.5	0.015	0.60	0.017	0.02	3%

The average time period decreases with the pivot to center-of-mass distance for the first three and increases for the last two measurements, ranging between 0.73 s and 0.57 s. Absolute uncertainties are small, the biggest is seen at $d = 1.3$ cm $\pm$ 0.1 cm, due to a smaller number of measured oscillations (5).

In the next step the measured data points are fitted with a predicted function of Equation 18 with varying length of the rod *l* and shown in Figure 5 (experimental - blue line). The calculated value with measured length of the rod is also displayed (calculated - red line) and exibits the same qualitative pattern.

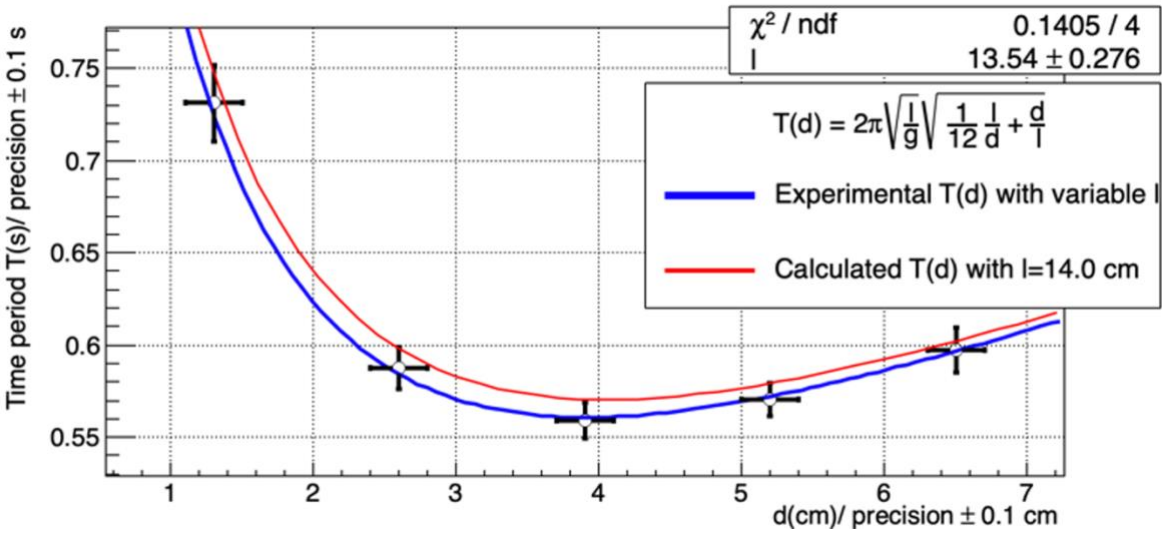

Figure 5: Best fit line of the time period: The best-fit line (blue) and the calculated time period (red) are shown.

The experimental rod length $l = 13.54$ cm $\pm$ 0.28 cm obtained from the blue fit line agrees well with the (measured) true length $l = 14.0cm \pm 0.1$ cm, from which the red line (calculated values) is drawn. To quantify the deviation, the %Error of the parameter l is calculated:

$$\%error = \left|\frac{experimental - true}{true}\right| \cdot 100 \qquad (20)$$

$$\%error = \left|\frac{13.5 - 14.0}{14.0}\right| \cdot 100$$

$$\%error = 3.3\%$$

Moreover, to quantify the difference between the measured and calculated (red line) values of time period, their $\%Error$ is calculated. First the true values of time period are calculated using the Equation (18). The calculations are shown for axis distance $6.5\ \text{cm} \pm 0.1\ \text{cm}$, and remaining values are written in Table 8.

1. Calculating the true value:

$$T = 2\pi \sqrt{\frac{0.140\ \text{m}}{9.81\ \text{m/s}^2}} \sqrt{\frac{0.140\ \text{m}}{12 \cdot 0.065\ \text{m}} + \frac{0.065\ \text{m}}{0.140\ \text{m}}} = 0.6022\ s = 0.60\ s$$

2. Calculating the %Error using average value as "experimental":

$$\%Error = \left|\frac{experimental - true}{true}\right| \cdot 100$$

$$\%Error = \left|\frac{0.597 - 0.602}{0.602}\right| \cdot 100 = 0.8\%$$

Table 8: Experimental value, calculated value and %error

$Axis\ distance\ d\ (cm)$ $\pm 0.1cm$	$T_{mean}\ (s)$ $\pm 0.1s$	$T_{calculated\ (s)}$	$\%Error$
1.3	0.73	0.75	2.1
2.6	0.59	0.60	1.8
3.9	0.56	0.57	2.0
5.2	0.57	0.58	1.5
6.5	0.60	0.60	0.8

Comparing the experimental and calculated time period results, the predicted values (red line) are slightly higher than the measured ones (Table 8, Figure 5). The table indicates a small %error, ranging between 0.8% and 2.1%. Again, the highest deviation is observed for the smallest distance. $d = 1.3cm$.

In Figure 6, the measured data are shown alongside the predicted function for time period *T(d), (*Equation 18), marked with a blue line, and the predicted time of the point-like mass pendulum (Equation 2), marked with red line. As expected, the time period of a compound pendulum approaches the time period of a point-like mass pendulum for large distances *d,* where the rigid body can be treated as a point-like. The position of the minimum time period is indicated, as determined from Equation 18 by finding the distance *d* at which the first derivative with respect to *d* is 0.

$$\left(\frac{l}{12d} + \frac{d}{l}\right)' = 0 \Longrightarrow x = \frac{d}{l}$$

$$\left(\frac{1}{12x} + x\right)' = 0$$

$$-\frac{1}{12x^2} + 1 = 0 \Longrightarrow x = \frac{1}{2\sqrt{3}} \Longrightarrow d = \frac{l}{2\sqrt{3}}$$

Inserting for distance $l = 14.0$ cm, the minimum point is found at distance:

$$d = \frac{14}{2\sqrt{3}} = 4.04\ \text{cm} = 4.0\ \text{cm}$$

It can be observed that the calculated value agrees with the measured minimal values.

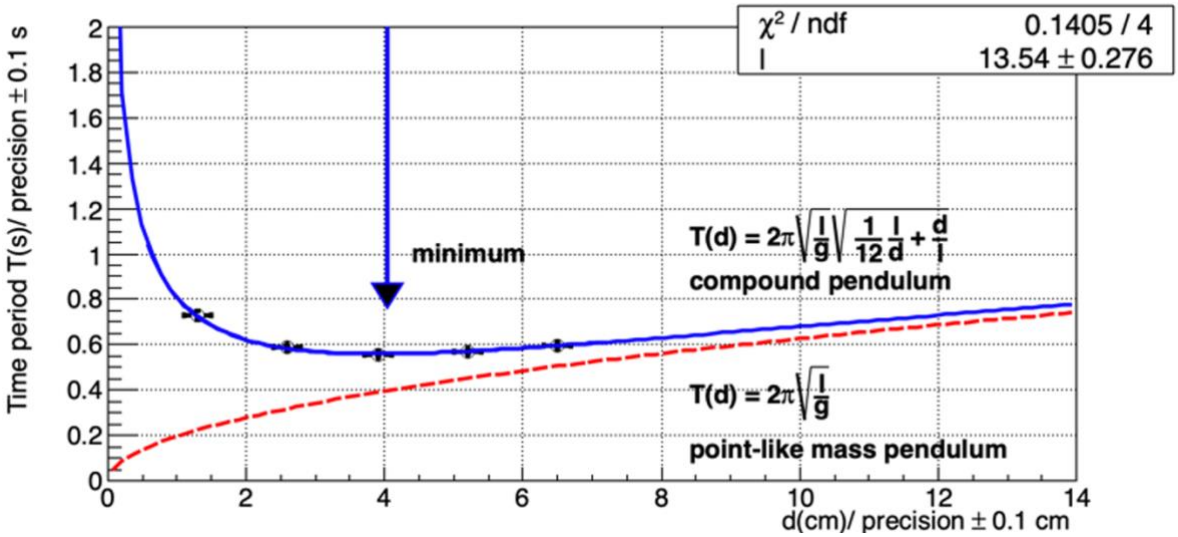

Figure 6: Period of oscillation for time period of a point mass and coupled pendulum in relationship with distance from the mass centre

6. CONCLUSION

This investigation evaluated how the increasing pivot to center-of-mass distance influences the time period of oscillation of the compound pendulum.

At the start of this investigation, it has been derived using the Newton's law and an expression for the moment of inertia for a rigid body-rod, that its oscillation time period depends on the length of the rod *l* and the pivot to center-of-mass distance *d,* proportionally to $\sqrt{\frac{l^2}{12d} + d}$ (see Equation 19). The theoretically derived equation exhibits minumum as suggested in the first hypothesis.

The conducted measurements also supported this hypothesis: they showed decrease in the oscillation period for the first three pivot to center-of-mass distances (*1.3* cm*, 2.6* cm*, 3.9* cm*)* and after reaching a minimum at d = 4.0 cm the time period increased again (Figure 5).
It was concluded that the measurements provided reasonably accurate predictions, since the combined equipment uncertainties were lower than 10%. When evaluating the precision of the measurements, the uncertainties ranged between 0.1 s and 0.3 s, and were most likely the result of a random error when stopping the stopwatch. The biggest uncertainty was denoted at the smallest axis distance, and emerged due to dispersion of the uncertainty over a smaller time (of only five oscillations). All uncertainties were small compared to the measured data which confirmed the precision and reliability of the results; unexpectedly since the method (relying on observations) isn't usually considered as reliable.

Lastly, it has also been established in support to the second hypothesis, that after reaching the minimum point, the function describing the relationship between the oscillation period and pivot to center-of-mass distance, approaches the function for a simple point-like mass pendulum (Figure 6).
Moreover, the theoretical function of Equation 18 which was fitted to the results, allowed for the extraction of the parameter l, corresponding to the measured values. It was identified that

the extracted length was $l = 13.5\ \text{cm} \pm 0.3\ \text{cm}$. When comparing it to the true value of the rod $d = 14.0\ \text{cm} \pm 0.1\ \text{cm}$, a 3% error was calculated.
This was also further confirmed by comparison of each measurement to its theoretical value using Equation 18. All the measurements showed deviations between 0.8% and 2.1% from the theoretically predicted value, and so all the results were deemed accurate.

7. EVALUATION

7.1 WEAKNESSES

Distance range: The experiment was conducted at pivots positioned inside the rigid body-the rod. After the turning point, there was only one more distance at which the measurements were acquired. Therefore, results were insufficient as they mostly showed the behavior of the decreasing time period and not for the complete rigid body's behaviour in the increasing time period range.
Variations in the maximum positions of the oscillations: Recording the measurements based on a qualitative observations of when an oscillation has ended, introduced random errors.
Oscillation count for distance d=1.3cm: For the smallest distance of the axis, only five oscillations were recorded. This led to an increased random error. The random fluctuations in timing measurements became more evident, as the oscillation time was shorter.
Pivot friction: The friction between the axis and the rod could have affected the time period as the steel pole was not round but rectangular. This introduced random error, depending on how the pole was positioned.
Rod imperfections: At the start of the experiment, it was predicted that the mass was uniformly distributed and the center-of-mass was determined. However, the rod is a homogeneous rod of length of 14 cm with eleven holes distributed alongside its length, and the rod could have deviations in the mass distribution, leading to systematic errors.
Oscillation damping: In this experiment, the oscillation damping was not considered in the calculations. Note that the derived formulas only apply to the undamped
oscillations. Here, especially for the d=1.3cm, where the motion was terminated after five oscillations, damping significantly affected the time period and introduced a systematic error in the measurement.

7.2 STRENGHTS

Release angle: each time a measurement was made, the mass was released from the same small angle, which was ensured by measuring the angle of release. Since the derived equations only apply for small angles, the measurements were more accurate this way.
Multiple measurements: The experiment comprised ten trials for each axis distance, which reduced the random errors and ensured reliability of the results.
Measurement of multiple oscillations. The time of several oscillations was measured, and afterwards converted to the time period of one oscillation. This way the random error was reduced, as the uncertainty due to stopping variations dispersed over a larger time.

7.3 IMPROVEMENTS

If the experiment were conducted again, some changes would be imposed. Firstly, a different range would be chosen, to include distances after the turning point, which would show an increase in the time period. Next to reduce the damping, the friction in the pivot would be reduced by choosing a round pivot instead of a non-uniform rectangular one. Thirdly, a more precise equipment, not relying on the qualitative observations, could be used, to ensure even greater precision and accuracy.

7.4 EXTENSION:

An extension of this experiment could involve investigating how the different shapes of rigid bodies influence the time period. In this experiment, the rigid body was a rectangle; however, different shapes would have different moments of inertia, which would lead to different results.

Moreover, it could also be investigated how the time period changes for a body which is not homogeneous.

8. BIBLIOGRAPHY

"Brian Law's woodenclocks - Clock 32 with compound pendulum". *YouTube*. https://www.youtube.com/watch?v=q7NaEoRTJR4. Accessed: 7. Mar. 225.

"Compound Pendulum." *Britannica*. https://www.britannica.com/technology/compound-pendulum. Accessed: 4 Mar. 2025.

"Compound Pendulum Experiment." *Virtual Labs - Amrita University*. vlab.amrita.edu/index.php?sub=1&brch=280&sim=210&cnt=2. Accessed: 4 Mar. 2025.

"Determining g Using a Compound Pendulum." *Aleph Science*. https://alep.science/content/labs/B5-1%20Determining%20g%20Using%20a%20Compound%20Pendulum.html. Accessed: 4 Mar. 2025.

"Inertial Moments." *University of Oldenburg*. https://uol.de/f/5/inst/physik/ag/physikpraktika/download/GPR/pdf/E_Traegheitsmomente.pdf . Accessed: 4 Mar. 2025.

Mujtaba, Abid. "Compound Pendulum." *PHY-108 Lab Manuals*. https://abid-mujtaba.github.io/phy-108-lab-manuals/docs/compound-pendulum.pdf. Accessed: 4 Mar. 2025.

"Moment of inertia." *Toppb. https://www.toppr.com/guides/physics/system-of-particles-and-rotational-dynamics/moment-of-inertia/.* Accessed on: 3. Mar. 2025

"Steiner's Theorem." *Solver Edu*. https://solveredu.com/en/post/steiner-s-theorem/. Accessed: 4 Mar. 2025.